



# Heterogeneous azide–alkyne cycloaddition in the presence of a copper catalyst supported on an ionic liquid polymer/silica hybrid material

Klaudia Fehér<sup>1</sup> | Enikő Nagy<sup>1</sup> | Péter Szabó<sup>2†</sup> | Tatjana Juzsakova<sup>3</sup> | Dávid Srankó<sup>4</sup> | Ágnes Gömöröy<sup>5</sup> | László Kollár<sup>6</sup> | Rita Skoda-Földes<sup>1</sup>

<sup>1</sup>Department of Organic Chemistry, University of Pannonia, Institute of Chemistry, Egyetem u. 10 (PO Box 158), H-8200 Veszprém, Hungary

<sup>2</sup>Department of Analytical Chemistry, University of Pannonia, Institute of Chemistry, Egyetem u. 10 (PO Box 158), H-8200 Veszprém, Hungary

<sup>3</sup>University of Pannonia, Institute of Environmental Engineering, Egyetem u. 10 (PO Box 158), H-8200 Veszprém, Hungary

<sup>4</sup>Department of Surface Chemistry and Catalysis, Hungarian Academy of Sciences, Centre for Energy Research, PO Box 49, H-1525, Budapest 114, Hungary

<sup>5</sup>Research Centre for Natural Sciences, Hungarian Academy of Sciences, Magyar tudósok körútja 2, H-1117 Budapest, Hungary

<sup>6</sup>Department of Inorganic Chemistry and MTA-PTE Research Group for Selective Chemical Syntheses, University of Pécs, Ifjúság u. 6 (PO Box 266), H-7624 Pécs, Hungary

## Correspondence

Rita Skoda-Földes, University of Pannonia, Institute of Chemistry, Department of Organic Chemistry, Egyetem u. 10 (PO Box 158), H-8200 Veszprém, Hungary.  
Email: skodane@almos.uni-pannon.hu

## Present Address

<sup>†</sup>Applied Physics, Division of Materials Science, Department of Engineering Science and Mathematics, Luleå University of Technology, 97187 Luleå, Sweden

## Funding information

European Union - European Regional Development Fund, Grant/Award Number: GINOP-2.3.2-15-2016-00049; National Research, Development and Innovation Office, Grant/Award Numbers: OTKA K120014 and OTKA K105632; New National Excellence Program of the Ministry of Human Capacities, Grant/Award Number: ÚNKP-16-2-II

Heterogeneous copper catalysts were prepared by the deposition of CuI on a hybrid material consisting of silica and a polymer with imidazolium moieties. The solid materials were characterised using solid-phase NMR, Fourier transform infrared, Raman and X-ray photoelectron spectroscopies and Brunauer–Emmett–Teller measurements. The formation of copper–carbene complexes was proved from Raman spectra and the results were supported by density functional theory calculations. The catalyst could be recycled efficiently with low loss of copper. Metal leaching was proved to be facilitated by the use of conditions typical for a homogeneous system (the presence of a polar solvent or the addition of a tertiary amine). Besides simple model reactions, the best catalyst was found to be suitable for the synthesis of triazoles of more elaborate structure, such as ferrocene or steroid derivatives.

## KEYWORDS

CuAAC reaction, DFT calculations, Raman spectroscopy, recyclability, triazole

## 1 | INTRODUCTION

Copper-catalysed azide–alkyne cycloaddition (CuAAC) has been one of the most widely used catalytic reactions in organic synthesis. It was reported independently by Sharpless and co-workers<sup>[1]</sup> and Meldal and co-workers<sup>[2]</sup>

in 2002 and there is still intense ongoing research involving the improvement of the methodology.

The popularity of the CuAAC reaction, the most widely used representative of the so-called ‘click’ reactions<sup>[3]</sup> is mainly due to its robustness, selectivity, functional group tolerance and biocompatibility that

make it a versatile tool in medicinal chemistry,<sup>[4]</sup> bioconjugation<sup>[5]</sup> and supramolecular chemistry.<sup>[6]</sup>

Under homogeneous conditions, a great variety of copper precursors have been used. The possibilities include the application of Cu(I) compounds together with a stabilising ligand or Cu(II) salts in the presence of a reducing agent to obtain the catalytically active Cu(I) species.<sup>[7]</sup>

One of the main limitations of homogeneous CuAAC reactions is the presence of a significant amount of toxic copper complexes in the end products. Therefore, various strategies for catalyst removal have been reported.<sup>[8]</sup> The advantage of these methods lies not only in obtaining products with higher purity but also in offering the possibility of catalyst recirculation. The application of ionic liquids as solvents combines the benefits of homogeneous and heterogeneous reactions. A homogeneous reaction takes place in the ionic liquid phase but the products can easily be isolated via extraction and the solvent/catalyst mixture can be recycled.<sup>[9]</sup> However, this methodology has some drawbacks, such as the relatively high price of the ionic liquids or difficulties in their handling due to their high viscosity. Another solution is the use of copper nanostructures<sup>[10]</sup> that usually have high catalytic activity but can be recovered only by centrifugation<sup>[11,12]</sup> or by the deposition of the active species on magnetic nanoparticles,<sup>[13,14]</sup> facilitating separation by the use of an external magnet. Still, in some cases, efficient recirculation of the catalyst can be achieved only under strictly inert conditions (in a glovebox) that should be used to avoid facile oxidation of Cu(I).<sup>[13]</sup> Excellent results can be obtained by coating the magnetic nanoparticles with stabilising ligands, such as 1,3-di(adamantyl)imidazole, which ensures small loss of copper (3% of the original load) and high activity retained in nine cycles.<sup>[15]</sup>

Besides some rare examples of special copper complexes, e.g. Cu(I)(tris(2-dioctadecylaminoethyl)amine)Br that shows unusual solubility-based thermomorphic properties in polar solvents that allows recovery of the active form by simple filtration,<sup>[16]</sup> the most prevailing solution for effective catalyst recycling is the immobilisation of the active species on a solid support, such as charcoal,<sup>[17,18]</sup> graphene oxide,<sup>[19]</sup> alumina,<sup>[20]</sup> clays<sup>[21,22]</sup> or organic/inorganic hybrid materials.<sup>[23,24]</sup> Among them, SiO<sub>2</sub> with grafted imidazolium cations<sup>[24]</sup> was proved to be an excellent support, resulting in a stable catalyst that could be used several times under solvent-free conditions. Biopolymers, such as chitosan,<sup>[25,26]</sup> and synthetic polymers decorated with suitable ligands to stabilise the copper catalyst<sup>[27–35]</sup> are also suitable supports. However, a noticeable decrease of catalytic activity was observed after the third or fourth run in many cases.<sup>[18,21–23,26,32]</sup> Excellent results in catalyst recycling were reported with polymers incorporating special organic moieties,

such as a tetradentate Schiff base ligand,<sup>[34]</sup> tris(benzyltriazolylmethyl)amine,<sup>[28]</sup> (benzimidazolylmethyl)-bis(pyridylmethyl)amine<sup>[31]</sup> and dimethylaminomethyl groups,<sup>[27]</sup> as well as quaternary ammonium<sup>[29]</sup> or imidazolium ions.<sup>[35]</sup> At the same time, these catalysts were evaluated mainly in the cycloaddition reactions of azides and alkynes with simple aliphatic and aromatic moieties, with the exception of some carbohydrates<sup>[29,36]</sup> and a single example for a steroid derivative.<sup>[17]</sup>

As part of our ongoing interest in the functionalisation of ferrocene<sup>[37]</sup> and steroid derivatives<sup>[38,39]</sup> using click chemistry, we wanted to explore the possibility of using immobilised copper catalysts for the CuAAC reactions of such compounds. Ferrocenetriazole derivatives were proved to be electrochemically detectable receptors for anions, cations and ion pairs.<sup>[40]</sup> Steroids bearing triazolyl moieties often exert biological activity that renders them interesting targets in pharmaceutical chemistry.<sup>[41]</sup>

In the present paper, we report the application of an inorganic/organic hybrid material composed of silica and a polymer of 1-methyl-3-(4-vinylbenzyl)imidazolium chloride as an excellent support for CuAAC reactions of simple alkynes and azides. The performance of the catalyst in cycloadditions of ferrocene and steroid derivatives was found to depend strongly on the steric properties of the starting materials.

## 2 | EXPERIMENTAL

<sup>1</sup>H NMR and <sup>13</sup>C NMR spectra were recorded in CDCl<sub>3</sub>, deuterated dimethylsulfoxide (DMSO-*d*<sub>6</sub>) and D<sub>2</sub>O with a Bruker Avance III 500 spectrometer at 500 and 125.7 MHz, respectively. GC–MS analysis was carried out with a Shimadzu GC–MS-QP2010SE instrument. High-resolution mass spectra of 17 $\alpha$ -(1-benzyl-1*H*-1,2,3-triazol-4-yl)estradiol (**7ad**) and 17 $\alpha$ -(1-ferrocenylmethyl-1*H*-1,2,3-triazol-4-yl)estradiol (**7bd**) were obtained using a Q-TOF Premier mass spectrometer (Waters Corporation, Milford, MA, USA) in positive electrospray ionisation mode.

Fourier transform infrared (FT-IR) spectra of cycloaddition products were obtained using a Thermo Nicolet Avatar 330 FT-IR instrument. Samples were prepared as KBr pellets. Elemental analyses were conducted with a 1108 Carlo Erba apparatus. Copper content of the catalysts and metal leaching values were determined using inductively coupled plasma atomic emission spectroscopy (ICP-AES). Conversions were calculated from GC measurements carried out with a Hewlett Packard (HP4890D) gas chromatograph using ferrocene as internal standard.

FT-IR spectra for the surface analysis of catalysts were measured using a Bruker Vertex 70 spectrometer with a Bruker Platinum ATR adapter without sample

preparation. The spectra were recorded at a resolution of  $2\text{ cm}^{-1}$  with a room temperature DTGS detector and 1024 scans were co-added. Raman spectra were obtained with a Bruker SENTERRA Raman microscope. The laser source was a green semiconductor laser (532 nm) with a maximum power of 10 mW. For the microscope, a 20 $\times$  objective was used. The Raman signal was collected with a thermoelectrically cooled charge-coupled device detector and recorded for typically 20 scans. A typical integration time for recording the Raman spectra was 30 s on average. The spectral resolution was  $4\text{ cm}^{-1}$ . Density functional theory (DFT) with B3LYP and PBE0 functional and LANL2DZ basis set was used for geometry optimisation and frequency analysis of [Cu(DMim)]I (DMim = *N,N'*-dimethylimidazol-2-ylidene), used as a model for the vibrational analysis of Cu-carbenes on the ground-state (singlet spin state) potential energy surface. All calculations were performed using the Gaussian 09 program.

Surface composition of fresh and spent catalysts was determined using X-ray photoelectron spectroscopy (XPS) performed with a KRATOS XSAM 800 XPS machine equipped with an atmospheric reaction chamber. Al  $K\alpha$  characteristic X ray line, 40 eV pass energy (energy steps of 0.1 eV) and FAT mode were applied for recording the XPS lines of Cu 2p, Cu LMM, O 1 s, N 1 s, C 1 s and Si 2p. C 1 s binding energy at 284.8 eV was used as reference for charge compensation. The surface concentrations of the elements were calculated from the integral intensities of the XPS lines using sensitivity factors given by the instrument manufacturer.

The specific surface area, pore volume and pore size distribution in micropore (1.7–2 nm), mesopore (2–50 nm) and macropore (50–100 nm) diameter ranges of silica and support **4** were determined using nitrogen adsorption/desorption at  $-196\text{ }^\circ\text{C}$  measured with a Micromeritics ASAP 2000-type instrument on samples previously outgassed overnight in vacuum at  $60\text{ }^\circ\text{C}$ . The surface areas of the samples ( $S_{\text{BET}}$ ) were determined using the Brunauer–Emmett–Teller (BET) method from the nitrogen adsorption isotherm. The pore volume values were calculated from the nitrogen desorption isotherms using the Barrett–Joyner–Halenda (BJH) theory.

## 2.1 | Preparation of 1-Methyl-3-(4-vinylbenzyl)-1*H*-imidazolium Chloride (**3**)<sup>[42]</sup>

In a Schlenk tube, 1-methylimidazole (**1**; 1.7 mmol, 135.5  $\mu\text{l}$ ), 4-vinylbenzyl chloride (**2**; 1.75 mmol, 246.6  $\mu\text{l}$ ) and dichloromethane (10 ml) were refluxed under inert atmosphere at  $60\text{ }^\circ\text{C}$  for 5 h. The solvent was evaporated under reduced pressure. The product was washed with diethyl ether and dried *in vacuo*. Ionic liquid **3** was

formed as a yellow viscous liquid (yield: 94%). Its NMR data corresponded well to those reported in the literature.<sup>[42]</sup>

$^1\text{H}$  NMR ( $\text{D}_2\text{O}$ ,  $\delta$ , ppm): 8.65 (s, 1H); 7.45 (d,  $J = 7.9\text{ Hz}$ , 2H); 7.36 (brs, 1H); 7.34 (brs, 1H); 7.29 (d,  $J = 7.9\text{ Hz}$ , 2H); 6.69 (dd,  $J = 11.0\text{ Hz}$ , 17.5 Hz, 1H); 5.79 (d,  $J = 17.5\text{ Hz}$ , 1H), 5.28 (s, 2H,  $\text{CH}_2$ ); 5.27 (d,  $J = 11.0\text{ Hz}$ , 1H); 3.78 (s, 3H,  $\text{CH}_3$ ).  $^{13}\text{C}$  NMR ( $\text{D}_2\text{O}$ ,  $\delta$ , ppm): 138.4; 135.9 (2C); 133.2; 129.0; 127.0; 123.8; 122.3; 115.5; 52.6; 35.8.

## 2.2 | Preparation of Support **4**

Ionic liquid monomer **3** (400 mg), silica (1.00 g, particle size 60–200  $\mu\text{m}$ , pre-treated by heating for 8 h at  $220\text{ }^\circ\text{C}$ ), dichloromethane (5 ml) and 5 mg of azobisisobutyronitrile were refluxed under an inert atmosphere at  $60\text{ }^\circ\text{C}$  for 5 h. The solvent was removed *in vacuo*. Then 8 ml of acetonitrile was added, the mixture was refluxed for 5 h and then the solvent was removed. This procedure was repeated five times and then the solid phase was filtered and dried under reduced pressure to afford 1.2 g of support **4** as an off-white powder.

## 2.3 | Preparation of Catalysts CAT-1–CAT-4

CAT-1: a mixture of **4** (120 mg), CuI (0.14 mmol, 26 mg) and 4 ml of acetonitrile–dimethylformamide (1,1) was stirred under inert atmosphere for 24 h. The solid material was filtered off under an inert atmosphere, washed with acetone, methanol, tetrahydrofuran (THF) and diethyl ether, and dried under reduced pressure. The catalyst was obtained as a pale green solid.

CAT-2–CAT-4: a mixture of **4** (120 mg), CuI (0.2 mmol, 38 mg for CAT-2, 0.1 mmol, 19 mg for CAT-3, 0.05 mmol, 10 mg for CAT-4), *t*BuOK (0.2 mmol, 22.4 mg) and THF (1 ml) was stirred under an inert atmosphere for 4 h. The solid material was filtered off under inert atmosphere, washed with cold methanol, acetone–methanol (1,1) and acetone, and dried under reduced pressure. Each catalyst was obtained as a pale green solid.

## 2.4 | General Procedure for CuAAC

A mixture of catalyst (with 0.01 mmol Cu content), 0.1 mmol of alkyne and 0.1 mmol of azide was stirred in  $\text{CH}_2\text{Cl}_2$  (1 ml) at room temperature under inert atmosphere until total conversion of the starting material could be detected by GC. The catalyst was allowed to settle and then the solution was removed using a syringe. The catalyst was reused without any treatment; a new portion of the reactants and the solvent were added. The

cycloaddition was carried out in 3–10 consecutive runs. The products were purified by column chromatography (silica; eluent: toluene–EtOAc).

## 2.5 | Characterisation of Products

1-Benzyl-4-phenyl-1*H*-1,2,3-triazole (**7aa**).<sup>[43]</sup> <sup>1</sup>H NMR (CDCl<sub>3</sub>, δ, ppm): 7.80 (dd, *J* = 8.5 Hz, 1.3 Hz, 2H); 7.66 (s, 1H); 7.41–7.36 (m, 5H); 7.33–7.30 (m, 3H); 5.57 (s, 2H, —CH<sub>2</sub>). <sup>13</sup>C NMR (CDCl<sub>3</sub>, δ, ppm): 148.2; 134.7; 130.6; 129.2; 128.8; 128.8; 128.2; 128.1; 125.7; 119.5; 54.2. FT-IR (KBr, cm<sup>-1</sup>): 1467; 1454; 1356; 1217; 1070; 1041; 764; 727; 690. MS (*m/z*/rel.int.): 235 (M<sup>+</sup>)/7; 206/19; 116/49; 91/52; 89/16; 65/13; 44/100; 39/11. Anal. Calcd for C<sub>15</sub>H<sub>13</sub>N<sub>3</sub> (%): C, 76.57; H, 5.57; N, 17.86. Found (%): C, 76.91; H, 5.42; N, 17.91. White solid; m.p. 124–127 °C; yield 99%.

Methyl 1-benzyl-1*H*-1,2,3-triazole-4-carboxylate (**7ab**).<sup>[43]</sup> <sup>1</sup>H NMR (CDCl<sub>3</sub>, δ, ppm): 7.97 (s, 1H); 7.42–7.36 (m, 3H); 7.31–7.27 (m, 2H); 5.57 (s, 2H); 3.92 (s, 3H). <sup>13</sup>C NMR (CDCl<sub>3</sub>, δ, ppm): 161.1; 140.3; 133.7; 129.3; 129.2; 128.3; 127.3; 54.5; 52.2. FT-IR (KBr, cm<sup>-1</sup>): 1723; 1536; 1454; 1430; 1336; 1225; 1045; 1017; 776; 715; 694. MS (*m/z*/rel.int.): 217 (M<sup>+</sup>)/1; 174/14; 130/21; 91/100; 65/19. Anal. Calcd for C<sub>11</sub>H<sub>11</sub>N<sub>3</sub>O<sub>2</sub> (%): C, 60.82; H, 5.10; N, 19.34. Found (%): C, 60.71; H, 5.32; N, 19.45. White solid; m.p. 99–102 °C; yield 78%.

(1-Benzyl-1*H*-1,2,3-triazol-4-yl)methyl acetate (**7ac**).<sup>[44]</sup> <sup>1</sup>H NMR (CDCl<sub>3</sub>, δ, ppm): 7.51 (s, 1H); 7.37–7.33 (m, 3H); 7.27–7.26 (m, 2H); 5.50 (s, 2H); 5.16 (s, 2H); 2.03 (s, 3H). <sup>13</sup>C NMR (CDCl<sub>3</sub>, δ, ppm): 170.8; 143.2; 134.4; 129.1; 128.9; 128.2; 123.6; 57.6; 54.2; 20.9. FT-IR (KBr, cm<sup>-1</sup>): 1740; 1454; 1433; 1225; 1053; 1033; 760; 719. MS (*m/z*/rel.int.): 231 (M<sup>+</sup>)/2; 188/11; 92/13; 91/100; 65/25; 43/58; 39/12. Anal. Calcd for C<sub>12</sub>H<sub>13</sub>N<sub>3</sub>O<sub>2</sub> (%): C, 62.33; H, 5.67; N, 18.17. Found (%): C, 62.41; H, 5.83; N, 18.22. Colourless oil; yield 71%.

17α-(1-Benzyl-1*H*-1,2,3-triazol-4-yl)estradiol (**7ad**).<sup>[45]</sup> <sup>1</sup>H NMR (DMSO-*d*<sub>6</sub>, δ, ppm): 8.97 (s, 1H); 7.89 (s, 1H); 7.40–7.37 (m, 2H); 7.35–7.31 (m, 3H); 6.96 (d, *J* = 8.5 Hz, 1H); 6.47 (dd, *J* = 8.5 Hz, 2.3 Hz, 1H); 6.42 (d, *J* = 2.3 Hz, 1H); 5.59 (d, *J* = 15.0 Hz, 1H); 5.56 (d, *J* = 15.0 Hz, 1H); 5.11 (s, 1H); 0.57–2.78 (m, 15 H, ring protons), 0.92 (s, 3H). <sup>13</sup>C NMR (DMSO-*d*<sub>6</sub>, δ, ppm): 155.4; 154.9; 137.6; 136.8; 130.9; 129.2; 128.5; 128.3; 126.5; 123.3; 115.4; 113.1; 81.6; 53.1; 48.1; 47.2; 43.7; 39.8; 37.7; 33.1; 29.7; 27.7; 26.5; 24.0; 14.8. FT-IR (KBr, cm<sup>-1</sup>): 1605; 1495; 1454; 1442; 1221; 1062; 1013; 866; 715. HRMS calculated for C<sub>27</sub>H<sub>32</sub>N<sub>3</sub>O<sub>2</sub> 430.2495 ([M + H]<sup>+</sup>), found 430.2496. White solid; m.p. 218–219 °C; yield 56%.

1-Ferrocenylmethyl-4-phenyl-1*H*-1,2,3-triazole (**7ba**). <sup>1</sup>H NMR (CDCl<sub>3</sub>, δ, ppm): 7.79 (dd, *J* = 8.3 Hz, 1.4 Hz, 2H); 7.64 (s, 1H); 7.41–7.38 (m, 2H); 7.30 (tt, *J* = 7.4 Hz,

1.2 Hz, 1H); 5.33 (s, 2H); 4.31 (t, *J* = 1.7 Hz, 2H); 4.23 (t, *J* = 1.7 Hz, 2H); 4.20 (s, 5H). <sup>13</sup>C NMR (CDCl<sub>3</sub>, δ, ppm): 147.7; 130.7; 128.8; 128.1; 125.7; 118.9; 80.8; 69.1; 69.0 (7C); 50.1. FT-IR (KBr, cm<sup>-1</sup>): 1462; 1332; 1221; 1103; 1070; 1050; 817; 764; 690. MS (*m/z*/rel.int.): 343 (M<sup>+</sup>)/43; 281/11; 253/11; 209/12; 208/16; 200/16; 199/95; 133/12; 121/100; 119/10; 96/17; 89/14; 73/13; 56/42; 44/21. Anal. Calcd for C<sub>19</sub>H<sub>17</sub>FeN<sub>3</sub> (%): C, 66.49; H, 4.99; N, 12.24. Found (%): C, 66.61; H, 5.05; N, 12.37. Yellow solid; m.p. 178–182 °C; yield 52%.

Methyl 1-ferrocenylmethyl-1*H*-1,2,3-triazole-4-carboxylate (**7bb**). <sup>1</sup>H NMR (CDCl<sub>3</sub>, δ, ppm): 7.96 (s, 1H); 5.34 (s, 2H); 4.27 (s, 2H); 4.24 (s, 2H); 4.19 (s, 5H); 3.91 (s, 3H, —OCH<sub>3</sub>). <sup>13</sup>C NMR (CDCl<sub>3</sub>, δ, ppm): 161.2; 139.8; 126.8; 79.8; 69.4; 69.0; 69.0; 52.1; 50.5. FT-IR (KBr, cm<sup>-1</sup>): 1724; 1536; 1454; 1430; 1336; 1225; 1046; 1017; 776; 715; 694. MS (*m/z*/rel.int.): 325 (M<sup>+</sup>)/6; 281/13; 253/10; 209/13; 208/17; 199/16; 191/9; 133/14; 121/15; 96/22; 73/22; 44/100. Anal. Calcd for C<sub>15</sub>H<sub>15</sub>FeN<sub>3</sub>O<sub>2</sub> (%): C, 55.41; H, 4.65; N, 12.92. Found (%): C, 55.32; H, 4.81; N, 12.71. Yellow solid; m.p. 169–171 °C; yield 93%.

(1-Ferrocenylmethyl-1*H*-1,2,3-triazol-4-yl)methyl acetate (**7bc**). <sup>1</sup>H NMR (CDCl<sub>3</sub>, δ, ppm): 7.49 (s, 1H); 5.27 (s, 2H); 5.15 (s, 2H); 4.27 (t, *J* = 1.6 Hz, 2H); 4.21 (t, *J* = 1.6 Hz, 2H); 4.17 (s, 5H); 2.03 (s, 3H). <sup>13</sup>C NMR (CDCl<sub>3</sub>, δ, ppm): 170.9; 142.7; 123.0; 80.6; 69.1; 69.0; 69.0; 57.6; 50.1; 20.9. FT-IR (KBr, cm<sup>-1</sup>): 1736; 1446; 1368; 1230; 1050; 813; 792. MS (*m/z*/rel.int.): 339 (M<sup>+</sup>)/25; 281/16; 208/16; 199/42; 191/9; 133/10; 121/42; 96/16; 73/20; 56/17; 44/100; 43/16. Anal. Calcd for C<sub>16</sub>H<sub>17</sub>FeN<sub>3</sub>O<sub>2</sub> (%): C, 56.66; H, 5.05; N, 12.39. Found (%): C, 56.77; H, 4.92; N, 12.55. Yellow solid; m.p. 74–76 °C; yield 92%.

17α-(1-Ferrocenylmethyl-1*H*-1,2,3-triazol-4-yl)estradiol (**7bd**). <sup>1</sup>H NMR (DMSO-*d*<sub>6</sub>, δ, ppm): 9.02 (s, 1H); 7.83 (s, 1H); 6.95 (d, *J* = 8.5 Hz, 1H); 6.47 (dd, *J* = 8.5 Hz, 2.3 Hz, 1H); 6.41 (d, *J* = 2.3 Hz, 1H); 5.28 (s, 2H); 5.12 (s, 1H); 4.35 (s, 1H); 4.32 (s, 1H); 4.18 (s, 7H); 0.59–2.76 (m, 15H, ring protons); 0.91 (s, 3H). <sup>13</sup>C NMR (DMSO-*d*<sub>6</sub>, δ, ppm): 155.4; 154.6; 137.6; 130.8; 126.4; 122.7; 115.4; 113.1; 83.3; 81.6; 69.1; 69.0; 69.0; 68.7; 49.2; 48.0; 47.1; 43.7; 39.8; 37.7; 33.1; 29.7; 27.7; 26.5; 24.0; 14.9. FT-IR (KBr, cm<sup>-1</sup>): 1609; 1503; 1442; 1287; 1234; 1053; 813. HRMS calculated for C<sub>31</sub>H<sub>35</sub>N<sub>3</sub>O<sub>2</sub>Fe 537.2079, found 537.2076. Yellow solid; m.p. 231–236 °C; yield 26%.

17α-Hydroxy-16β-(4-phenyl-1,2,3-triazol-1-yl)-5α-androstane (**7ca**).<sup>[39]</sup> <sup>1</sup>H NMR (CDCl<sub>3</sub>, δ, ppm): 7.81–7.80 (m, 3H); 7.40 (t, *J* = 7.4 Hz, 2H); 7.32 (t, *J* = 7.4 Hz, 1H); 4.63 (t, *J* = 8.8 Hz, 1H); 4.06 (brs, 1H); 2.78–2.98 (brs, 1H); 0.74–2.46 (m, 22 H); 0.93 (s, 3H, 18-H<sub>3</sub>); 0.81 (s, 3H, 19-H<sub>3</sub>). <sup>13</sup>C NMR (CDCl<sub>3</sub>, δ, ppm): 147.5; 130.6; 128.8; 128.1; 125.7; 119.6; 85.4; 70.2; 54.2; 49.4; 46.9; 44.5; 38.7; 36.4; 35.0; 32.7; 32.4; 31.9; 29.0; 28.9; 26.8; 22.2; 20.0; 18.0; 12.2. FT-IR (KBr, cm<sup>-1</sup>): 3423; 2917; 2848; 1458;

1385; 1225; 1074; 1053; 976; 764; 686. MS ( $m/z$ /rel.int.): 419 ( $M^+$ )/15; 391/11; 376/12; 173/19; 161/9; 148/12; 147/10; 146/22; 145/100; 144/18; 119/11; 117/14; 116/9; 109/24; 108/13; 107/10; 105/15; 104/25; 102/19; 95/20; 93/18; 91/20; 81/23; 79/19; 77/9; 67/29; 55/32; 44/17; 43/15; 41/19. Anal. Calcd for  $C_{27}H_{37}N_3O$  (%): C, 77.29; H, 8.89; N, 10.01. Found (%): C, 77.12; H, 9.01; N, 10.13. White solid; m.p: 232–234 °C; yield 46%.

17 $\alpha$ -Hydroxy-16 $\beta$ -(4-(methoxycarbonyl)-1*H*-1,2,3-triazol-1-yl)-5 $\alpha$ -androstane (**7cb**).<sup>[39]</sup>  $^1H$  NMR ( $CDCl_3$ ,  $\delta$ , ppm): 8.21 (s, 1H); 4.69 (t,  $J = 9.1$  Hz, 1H); 4.06 (brs, 1H); 3.93 (s, 3H); 3.04–3.31 (brs, 1H); 0.73–2.46 (m, 22 H, ring protons); 0.89 (s, 3H, 18- $H_3$ ); 0.81 (s, 3H, 19- $H_3$ ).  $^{13}C$  NMR ( $CDCl_3$ ,  $\delta$ , ppm): 161.2; 139.5; 127.3; 85.2; 70.4; 54.1; 52.1; 49.3; 46.9; 44.6; 38.6; 36.3; 34.9; 32.7; 32.3; 31.7; 28.9; 28.7; 26.7; 22.1; 19.9; 17.9; 12.1. FT-IR (KBr,  $cm^{-1}$ ): 3391; 2921; 2852; 1723; 1532; 1442; 1377; 1230; 1070; 1050; 817; 776. MS ( $m/z$ /rel.int.): 401 ( $M^+$ )/2; 358/11; 315/20; 314/73; 281/11; 275/14; 274/67; 259/27; 218/16; 203/18; 175/15; 161/10; 155/18; 154/13; 149/11; 148/24; 147/14; 135/16; 133/13; 128/50; 127/100; 122/12; 121/17; 119/13; 116/11; 110/16; 109/45; 108/30; 107/22; 105/20; 97/18; 96/69; 95/60; 94/15; 93/34; 91/30; 83/23; 82/13; 81/44; 80/12; 79/36; 77/15; 69/21; 68/25; 67/60; 57/10; 55/64; 54/9; 53/22; 44/27; 43/27; 41/45. Anal. Calcd for  $C_{23}H_{35}N_3O_3$  (%): C, 68.80; H, 8.79; N, 10.46. Found (%): C, 68.85; H, 8.57; N, 10.59. White solid; m.p. 182–188 °C; yield 79%.

16 $\beta$ -(4-(Acetoxymethyl)-1*H*-1,2,3-triazol-1-yl)-17 $\alpha$ -hydroxy-5 $\alpha$ -androstane (**7cc**).<sup>[39]</sup>  $^1H$  NMR ( $CDCl_3$ ,  $\delta$ , ppm): 7.66 (s, 1H); 5.19 (s, 2H); 4.59 (ddd,  $J = 8.4$  Hz, 7.2 Hz, 0.8 Hz, 1H); 4.02 (d,  $J = 0.8$  Hz, 1H); 2.44–2.59 (brs, 1H); 0.73–2.44 (m, 22 H); 2.06 (s, 3H); 0.90 (s, 3H, 18- $H_3$ ); 0.80 (s, 3H, 19- $H_3$ ).  $^{13}C$  NMR ( $CDCl_3$ ,  $\delta$ , ppm): 171.0; 142.6; 123.6; 85.3; 70.0; 57.7; 54.2; 49.3; 47.0; 44.5; 38.7; 36.4; 35.0; 32.8; 32.4; 31.9; 29.0; 28.8; 26.7; 22.1; 20.9; 20.0; 18.0; 12.2. FT-IR (KBr,  $cm^{-1}$ ): 3440; 2917; 2852; 1740; 1458; 1442; 1385; 1274; 1237; 1057; 1033; 829. MS ( $m/z$ /rel.int.): 415 ( $M^+$ )/2; 328/12; 327/28; 312/9; 284/20; 169/11; 148/10; 142/22; 135/12; 121/12; 110/12; 109/34; 108/14; 107/14; 105/16; 98/14; 96/13; 95/28; 93/28; 91/21; 84/12; 83/14; 82/35; 81/85; 80/49; 79/29; 77/10; 73/11; 70/10; 69/21; 68/31; 67/52; 57/13; 56/15; 55/58; 54/18; 53/14; 43/100; 41/40; 39/10. Anal. Calcd for  $C_{24}H_{37}N_3O_3$  (%): C, 69.37; H, 8.97; N, 10.11. Found (%): C, 69.12; H, 8.78; N, 10.01. White solid; m.p. 131–134 °C; yield 73%.

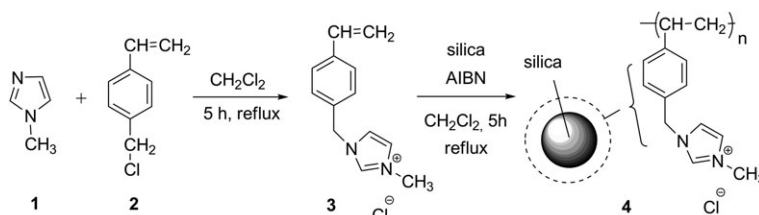
## 3 | RESULTS AND DISCUSSION

### 3.1 | Preparation and Characterisation of Catalysts

As polymers incorporating quaternary ammonium<sup>[29]</sup> and imidazolium ions<sup>[35]</sup> had been found to stabilise copper catalysts efficiently, copper was deposited on a support (**4**) obtained by the radical polymerisation of **3**, prepared by the reaction of **1** and **2** (Scheme 1).<sup>[42]</sup> During the first catalytic experiments, we encountered difficulties in the separation of the catalyst that could be recovered only by centrifugation. To solve this problem, polymerisation was carried out in the presence of silica gel. The process led to a solid material that could be removed from the reaction mixture by simple filtration or decantation. The solid material was characterised using  $^{13}C$  CP MAS NMR and FT-IR spectroscopies. The  $^{13}C$  CP MAS NMR spectrum (Figure 1) shows the presence of saturated carbon atoms in the region of 36–52 ppm and signals corresponding to carbon atoms of the phenyl and imidazolium rings between 124 and 146 ppm.

The values of the specific surface area ( $S_{BET}$ ) and pore volumes of silica and support **4** were determined from the experimental data of their nitrogen adsorption/desorption isotherms (Table 1). The silica used was a mesoporous material with pore size between 2 and 10 nm. This structure was preserved in support **4**. Although the BET surface area and total pore volume of the hybrid material **4** are lower than those of the original silica support due to deposition of the modifying material, no considerable change was observed in the average pore diameter after the polymerisation reaction.

Copper was immobilised on the surface of support **4** using CuI as the precursor. The catalysts were obtained in the absence (CAT-1) and in the presence of *t*BuOK (CAT-2–CAT-4; Table 2). This base had been used before during the preparation of similar catalysts to facilitate carbene formation from the imidazolium ion,<sup>[24,46]</sup> which might act as a ligand to form copper–N-heterocyclic carbene complexes. The copper content of the catalysts was determined by ICP-AES. In the presence of *t*BuOK, a higher amount of copper could be immobilised under identical conditions (Table 2; CAT-1 and CAT-2), so two



**SCHEME 1** Preparation of organic/inorganic hybrid support (**4**)

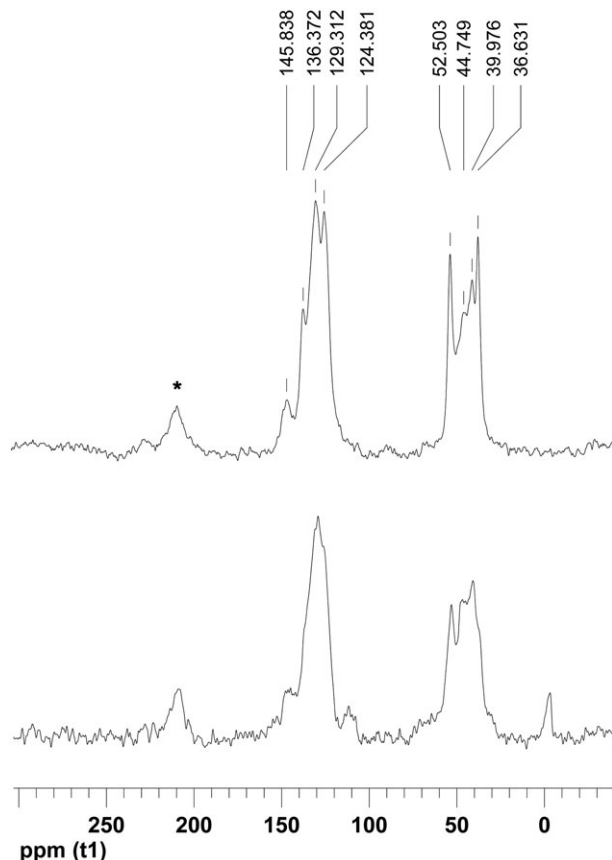


**FIGURE 1**  $^{13}\text{C}$  CP MAS NMR spectra of support **4** (above) and CAT-2 (below) (\* indicates a rotational sideband)

**TABLE 1** Surface area ( $S_{\text{BET}}$ ), pore volume ( $V$ ) and average pore diameter ( $D$ ) of silica and support **4**

	$S_{\text{BET}}$ ( $\text{m}^2 \text{g}^{-1}$ )	$V$ ( $\text{cm}^3 \text{g}^{-1}$ )	$D$ (nm) <sup>a</sup>
Silica	507	0.7162	4.66
Support <b>4</b>	291	0.4267	4.59

<sup>a</sup>BJH desorption average pore diameter.

**TABLE 2** Preparation of catalysts CAT-1–CAT-4<sup>a</sup>

Catalyst	CuI (mmol)	<i>t</i> BuOK	Cu content (mol%) <sup>b</sup>
CAT-1 <sup>c</sup>	0.2	–	3.5
CAT-2 <sup>d</sup>	0.2	+	10.3
CAT-3 <sup>d</sup>	0.1	+	3.1
CAT-4 <sup>d</sup>	0.05	+	1.2

<sup>a</sup>Reaction conditions: 120 mg support (**4**), CuI, 24 h, room temperature.

<sup>b</sup>Determined by ICP.

<sup>c</sup>Solvent:  $\text{CH}_3\text{CN}$ –dimethylformamide (1:1) (4 ml).

<sup>d</sup>Solvent: THF (1 ml), *t*BuOK (0.2 mmol).

catalysts with lower copper content (CAT-3 and CAT-4) were also prepared.

Except for some broadening of the signals, the  $^{13}\text{C}$  CP MAS NMR spectra of the catalysts did not show any

change when compared to the spectrum of the silica/polymer hybrid material. As an example, the  $^{13}\text{C}$  CP MAS NMR spectrum of CAT-2 is presented in Figure 1.

Poly(1-methyl-3-(4-vinylbenzyl)imidazolium chloride) (Pol), support **4** and CAT-1, obtained from CuI without the addition of *t*BuOK, as well as the catalyst with the lowest copper content (CAT-4) gave very similar FT-IR spectra (Figure 2). At the same time, a considerable broadening of bands could be observed in case of CAT-2, and a splitting of some of the bands corresponding to the imidazolium moiety (at 1450 and 1420  $\text{cm}^{-1}$ ) could be detected in the spectrum of CAT-3.

Surface composition of CAT-2 and CAT-3 was determined using XPS measurements (Tables 3 and 4). (The survey scans of the samples before and after the catalytic reaction are shown in Figure S2.) Strong lines related to oxygen, carbon and silicon are present in the spectra with weaker signs of copper, nitrogen, iodine and potassium.

The binding energy of the Si 2p peak was assigned to oxides (CAT-2: Si 2p<sub>3/2</sub> = 103.5 eV; CAT-3: Si 2p<sub>3/2</sub> = 102.9 eV).

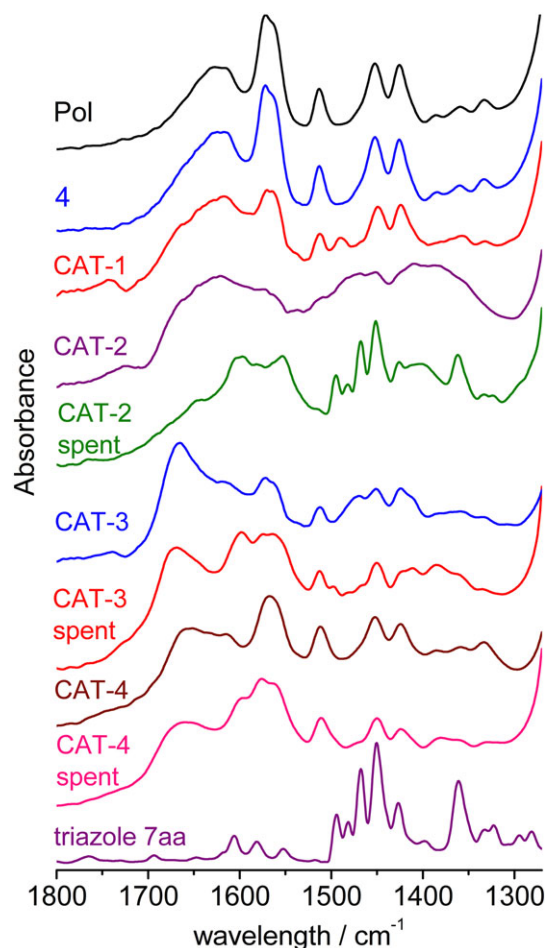


**FIGURE 2** FT-IR spectra of support **4** and fresh and spent catalysts (Pol: poly(1-methyl-3-(4-vinylbenzyl)imidazolium chloride) prepared in the absence of silica)

**TABLE 3** XPS surface composition of CAT-2

Element/component peak	Binding energy (eV)		Chemical state	Surface concentration (at.%)	
	Fresh	Spent		Fresh	Spent
Cu 2p	932.5	932.6	Cu(I)	1.6	1.5
	933.8	933.8	Cu(II)	10.5	6.0
I 3d	619.1	619.5	I <sup>-</sup>	1.1	0.9
O 1 s	530.6	530.8	Cu <sub>2</sub> O, CuO, O=C	15.6	9.1
	532.8	533.1	SiO <sub>2</sub> (C-OH (aliphatic))	33.3	39.5
N 1 s	400.8	401.4	Organic nitrogen species	3.6	4.0
C 1 s	284.8	284.8	C-C, C-H	15.9	15.9
	283.0	283.2	C-Cu (C-O-Cu)	3.7	3.0
	286.4	286.4	C-O, C-N, C=N	1.3	6.1
K 2p	292.9	292.9	K <sup>+</sup>	0.7	0.6
Si 2p	103.5	103.5	SiO <sub>2</sub>	12.6	13.2

**TABLE 4** XPS surface composition of CAT-3

Element/component peak	Binding energy (eV)		Chemical state	Surface concentration (at.%)	
	Fresh	Spent		Fresh	Spent
Cu 2p	932.9	932.9	Cu(I)	0.2	0.3
	934.0	934.0	Cu(II)	3.9	2.3
I 3d	619.1	619.0	I <sup>-</sup>	0.2	0.1
O 1 s	530.6	530.1	Cu <sub>2</sub> O, CuO, O=C	9.0	4.6
	532.5	532.6	SiO <sub>2</sub> (C-OH (aliphatic))	48.4	49.8
N 1 s	400.6	400.7	Organic nitrogen species	2.9	2.9
C 1 s	284.8	284.8	C-C, C-H	14.0	14.2
	282.5	282.9	C-Cu (C-O-Cu)	0.3	1.1
	286.5	286.3	C-O, C-N, C=N	3.2	5.1
K 2p	293.3	293.2	K <sup>+</sup>	1.0	0.9
Si 2p	102.9	103.2	SiO <sub>2</sub>	17.0	18.7

The surface modification did not cause major changes in chemical states.<sup>[46]</sup> The dominant part of the copper content was determined as Cu(II) chemical state by the position of the Cu 2p line at 933.8 eV and the presence of the characteristic ‘shake up’ satellite structure. The minor part of the copper can be either in Cu(0) or Cu(I) chemical state according to the line position at *ca* 932.5 eV.<sup>[47]</sup> Considerable amount of oxygen can be assigned to the SiO<sub>2</sub> phase with the O 1 s binding energy at *ca* 532.8 eV.<sup>[48]</sup> The spectral line appearing at lower binding energy of *ca* 530.6 eV is typical of C—O or oxygen in CuO state (*ca* 530.6 eV) but it can also be a mixture of oxygen in both Cu<sub>2</sub>O and CuO states.<sup>[49]</sup> The lines appearing at *ca* 619.1 eV are assigned to I 3d and therefore to the presence of iodine (*ca* 1 at.%).<sup>[47]</sup> It is assumed that

in spite of the inert conditions, some oxygen might have remained in the pores of silica gel that could not be removed completely. A small amount of potassium can be detected as well. While there seems to be a correlation between the amount of iodine and the Cu(I) ratio in the CAT-2 and CAT-3 samples (i.e. less copper and less iodine), there is no significant change in the amount of potassium with different copper loading. Due to the presence of the polymeric phase, there is a significant carbon content of the samples. The peak at 284.8 eV can be assigned to C—C/C—H bonds, while the peak at 286.4 eV is typical for carbon in C—O as well as for C—N and C—N bonds.<sup>[50–52]</sup> The peak appearing at *ca* 283 eV can be related to the formation of C—Cu (or C—O—Cu bonds by analogy with C—O—Ag in

metal–polymer composite<sup>[53]</sup>). There is also a correlation between the strength of the line at 283 eV and the copper content of the samples, i.e. the smaller the copper content the weaker the line appearing at 283 eV. Nitrogen content was detected at peak energies that are typical for an organic environment. The peak at *ca* 400.8 eV is assigned to N 1 s in organic nitrogen species.<sup>[54]</sup>

Although the formation of copper–N-heterocyclic carbene complexes could not be proved by <sup>13</sup>C NMR spectroscopy, possibly because of a low concentration in the sample, Raman measurements (Figure 3; Table 5) together with DFT calculations (Table 5) supported the presence of such species in the case of CAT-2. Upon comparing the spectra of CuI and CAT-2, considerable differences can be observed in the frequencies of Cu–I stretching (118 cm<sup>-1</sup> for CuI and 138 cm<sup>-1</sup> for CAT-2) and Cu–I bending (73 cm<sup>-1</sup> for CuI and 89 cm<sup>-1</sup> for CAT-2) indicating complexation.

An appreciable change can be detected in the frequencies involving vibrations of the imidazole moiety. (For comparison, Figure 3 includes the Raman spectra of the polymeric support and 1-methylimidazole.) Good agreement can be observed between the experimental data for CAT-2 and the calculated frequencies of a [Cu(DMim)]I complex. (Table 5 presents only the vibrations in which Cu is involved.) The most prominent peaks in the spectrum of CAT-2 correspond to Cu–C (Cu–carbene) stretching (above 1000 cm<sup>-1</sup>) and Cu–C (Cu–carbene) bending (below 1000 cm<sup>-1</sup>).

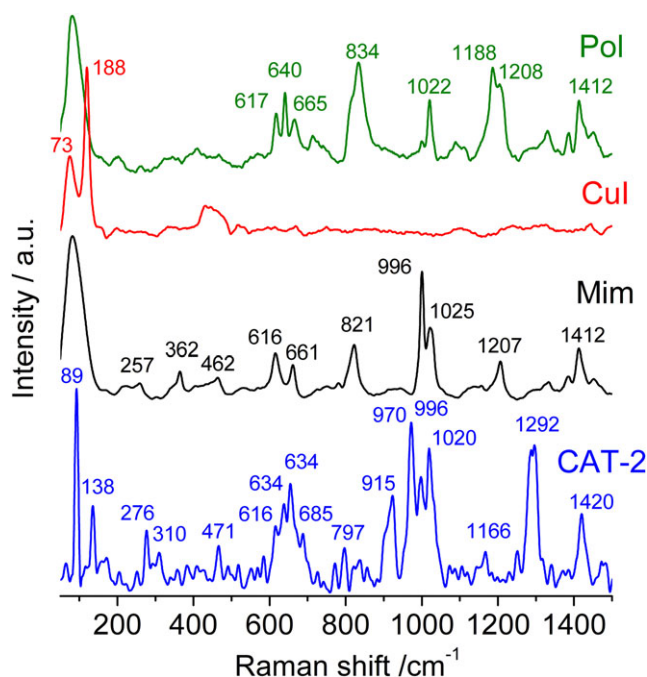


**FIGURE 3** Raman spectra of poly(1-methyl-3-(4-vinylbenzyl)imidazolium chloride) (Pol), CuI, 1-methylimidazole (Mim) and CAT-2

**TABLE 5** Experimental data obtained for CAT-2 sample and calculated frequencies of Raman-active modes of [Cu(DMim)]I

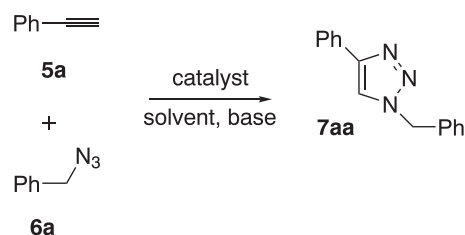
Raman-active mode <sup>a</sup>	Frequency (cm <sup>-1</sup> )		
	Experimental (CAT-2)	Calculated for [Cu(DMim)]I (B3LYP)	(PBE0)
$\nu_1$ (C)	138	145	147
$\nu_2$ (B)	276	270	274
$\nu_3$ (A)	310	355	362
$\nu_4$ (B)	471	453	459
$\nu_5$ (B)	634	611	627
$\nu_6$ (B)	685	672	669
$\nu_7$ (B)	797	747	764
$\nu_8$ (B)	970	1018	1035
$\nu_9$ (A)	1020	1114	1121
$\nu_{10}$ (A)	1166	1152	1168
$\nu_{11}$ (A)	1292	1348	1382
$\nu_{12}$ (A)	1420	1391	1426

<sup>a</sup>A: [Cu–imidazole] stretching; B: [Cu–imidazole] bending; C: [Cu–iodine] stretching.

### 3.2 | Catalytic Reactions

The catalysts were evaluated in the cycloaddition reaction of phenylacetylene (**5a**) with benzyl azide (**6a**) (Scheme 2). Reaction times required for quantitative conversion of substrate **5a** were estimated by GC. The results are summarised in Table 6.

Catalysts CAT-1 and CAT-2 showed similar catalytic activity under identical conditions (Table 6, entries 1–4). In the absence of the base, much longer reactions were necessary to achieve total conversion, but copper leaching decreased considerably. (Although the exact amount of copper in the filtrate was not determined in the first experiment (entry 1), the green colour of the reaction mixture clearly indicated a considerable loss of the metal.) As acetonitrile is a strongly coordinating solvent and may facilitate the loss of copper,<sup>[28]</sup> the possibility of using other reaction media was also taken into account. However, much lower conversion could be achieved in ethanol or THF, with conversions of 50 and 90%, respectively,



**SCHEME 2** Azide–alkyne cycloaddition of phenylacetylene (**5a**) with benzyl azide (**6a**)

**TABLE 6** Efficiency of catalysts in cycloaddition of phenylacetylene (**5a**) with benzyl azide (**6a**)<sup>a</sup>

Entry	Catalyst	Solvent	Base	Reaction time required for quantitative conversion (h)	Cu leaching (%) <sup>b</sup>
1	CAT-1	CH <sub>3</sub> CN	+	14	n.d.
2	CAT-1	CH <sub>3</sub> CN	–	48	8.7
3	CAT-2	CH <sub>3</sub> CN	+	17	8.2
4	CAT-2	CH <sub>3</sub> CN	–	48	4.3
5	CAT-2	CH <sub>2</sub> Cl <sub>2</sub>	–	96	0.8
6 <sup>c</sup>	CAT-2	CH <sub>2</sub> Cl <sub>2</sub>	–	72	3.7
7 <sup>d</sup>	CAT-2	CH <sub>2</sub> Cl <sub>2</sub>	–	7	11.5
8	CAT-3	CH <sub>2</sub> Cl <sub>2</sub>	–	24	<0.14

<sup>a</sup>Reaction conditions 0.1 mmol **5a**, 0.1 mmol **6a**, base (0.1 mmol DIPEA), catalyst (with 0.01 mmol Cu content), 1 ml solvent, room temperature.

<sup>b</sup>mol% of the original load of Cu, determined by ICP.

<sup>c</sup>0.1 mmol **5a**, 0.1 mmol **6a**, catalyst (with 0.02 mmol Cu content), 1 ml solvent, room temperature.

<sup>d</sup>Reflux.

after five days. A slow reaction took place also in dichloromethane with a total conversion only after four days (entry 5), but the amount of leached copper decreased noticeably.

An increase in the copper-to-substrate ratio (entry 6) and especially the use of a higher temperature (entry 7) led to a decrease in the necessary reaction time, but it was accompanied by a higher loss of copper. Both changes in the reaction conditions may lead to a higher concentration of copper nanoparticles in the liquid phase that may result in enhanced aggregation that might prevent resorption of the metal particles on the surface and lead to higher degree of leaching.

To achieve a better stabilisation of copper, a catalyst with a lower copper-to-support ratio was prepared (Table 2, CAT-3). In the presence of CAT-3, the starting materials were fully converted to the product (**7a**) in 24 h. Besides, copper leaching was below the detection limit (Table 6, entry 8). A further reduction in the amount of immobilised Cu (CAT-4, Table 2) led to a dramatic decrease in catalytic activity resulting in only 51% conversion after 120 h.

FT-IR spectra (Figure 2) and surface composition of spent catalysts (CAT-2, obtained from an experiment carried out according to Table 6, entry 5 (Table 3); CAT-3, obtained from an experiment carried out according to Table 6, entry 8 (Table 4)) were compared to the data for the freshly prepared ones. In the case of CAT-3, there is no change in the FT-IR spectrum after the catalytic reaction, but the presence of some triazole product can be detected in the spectrum of spent CAT-2. It is assumed that because of the higher copper content of this catalyst some Cu–triazole complexes might be formed. An increase in the amount of surface nitrogen species could be detected also by XPS (Table 3). Interestingly, a

considerable decrease in the surface concentration of Cu(II) could be noticed in the case of both catalysts. At the same time, ICP-AES data showed no change in the copper content of spent CAT-3 catalyst, indicating a rearrangement of the surface of the catalyst during the reaction. It should also be noted that the surface concentration of Cu(I) did not change considerably during the reaction with CAT-2 (Table 3) and even an increase could be observed in the case of CAT-3 (Table 4).

Presumably, the hard Pearson acid Cu(II) is able to enter the pores of silica (characterised as O-rich hard Pearson base ‘ligand surroundings’), while the soft Pearson acid Cu(I) is not. Cu(II) is expected to form more stable complexes with ‘hard’ silica than the ‘soft’ Cu(I).

To obtain information about the homogeneous or heterogeneous nature of the leached species, mercury poisoning tests were carried out for some reactions of CAT-2 and CAT-3 (Table 7). The catalytic mixtures were filtered after a couple of hours. One half of the mixture was stirred further and the other was treated similarly but in the presence of mercury. These experiments support the previous observation that both acetonitrile and *N,N*-diisopropylethylamine (DIPEA) facilitate the loss of metal. A marked increase in the conversion after the removal of the heterogeneous catalyst was observed in the absence of mercury (Table 7, entry 1), and some further reaction could be detected even in its presence (entry 2) showing that mainly copper nanoparticles but also some complexes have leached into the solution. Similar experiments with CAT-3 in CH<sub>2</sub>Cl<sub>2</sub> (entries 5 and 6) showed almost no conversion in the absence of the solid catalyst. These results are in accordance with the leaching data obtained by ICP measurements (Table 6, entries 2, 3 and 8).

TABLE 7 Mercury poisoning tests<sup>a</sup>

Entry	Catalyst	Solvent	Base	First step		Second step		
				Reaction time (h)	Yield of 7aa (%) <sup>b</sup>	Hg	Reaction time (h)	Yield of 7aa (%) <sup>b</sup>
1	CAT-2	CH <sub>3</sub> CN	DIPEA	2	37	–	22	99
2						+	22	47
3	CAT-2	CH <sub>3</sub> CN	–	5	17	–	21	51
4						+	21	37
5	CAT-3	CH <sub>2</sub> Cl <sub>2</sub>	–	5	35	–	19	35
6						+	19	35

<sup>a</sup>Reaction conditions: 0.1 mmol **5a**, 0.1 mmol **6a**, catalyst (with 0.01 mmol Cu content), 1 ml solvent, room temperature.

<sup>b</sup>Determined by GC.

The recyclability of CAT-3 was also tested in the model reaction. The progress of triazole formation was followed by GC using fresh and spent catalysts (Figure 4). The results show that even a slight increase in the reaction rate can be observed after the reuse of the catalyst.

During further recycling tests, some decrease in the catalytic activity was observed only after the seventh run (Figure 5) and somewhat longer reaction time had to be used to achieve total conversion in cycles 8–10. A total loss of 8% of the original load of copper was detected in the 10 cycles. The low level of copper leaching is in accordance with the hot filtration and mercury poisoning tests (Table 7, entries 5 and 6).

It should be mentioned that the activity of CAT-3 was also evaluated in the presence of sodium ascorbate (in a CH<sub>2</sub>Cl<sub>2</sub>–water (1,1) solvent mixture) to reduce surface-bonded Cu(II) to Cu(I). In a 20 h reaction, 80% conversion was achieved, which is considerably lower than that obtained under the standard conditions (95% after 20 h).

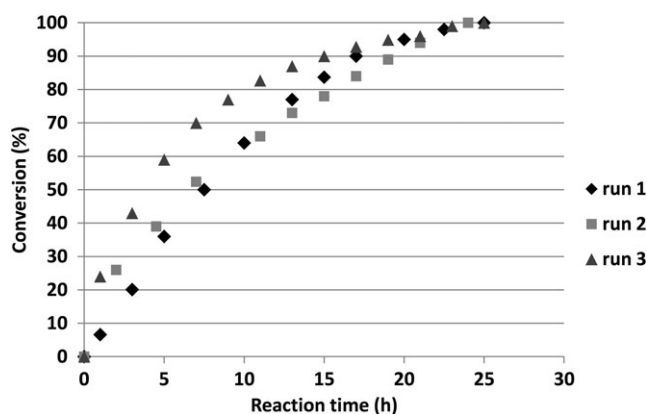


FIGURE 4 Triazole formation in the reaction of **5a** and **6a** in the presence of fresh and spent CAT-3 catalyst (reaction conditions: 0.1 mmol **5a**, 0.1 mmol **6a**, CAT-3 (with 0.01 mmol Cu content), 1 ml of CH<sub>2</sub>Cl<sub>2</sub>, room temperature)

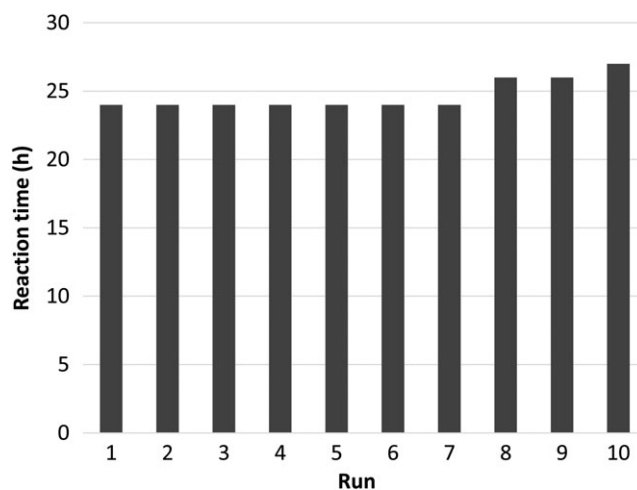
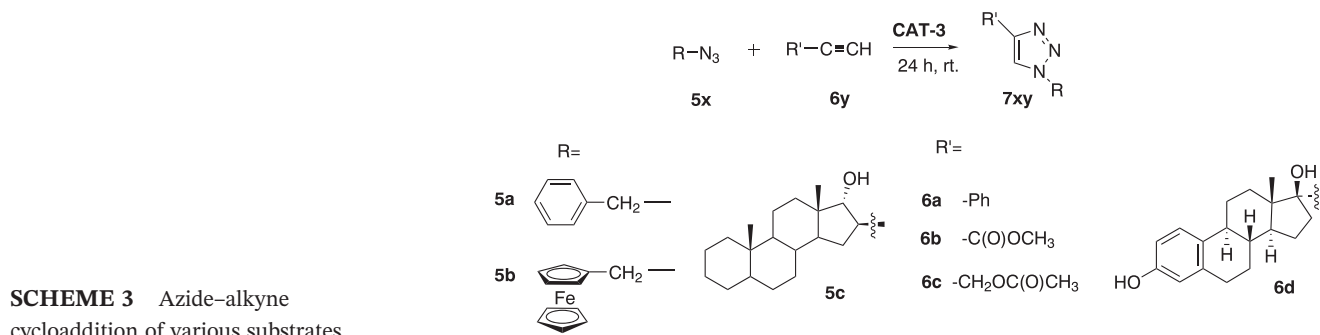


FIGURE 5 Recycling experiments with CAT-3: reaction time necessary for total conversion (reaction conditions: 0.1 mmol **5a**, 0.1 mmol **6a**, CAT-3 (with 0.01 mmol Cu content), 1 ml CH<sub>2</sub>Cl<sub>2</sub>, room temperature)

### 3.3 | Synthesis of Other 1,4-Disubstituted 1,2,3-Triazoles

Based on the experiments discussed above, CAT-3 was chosen to carry out CuAAC reactions of other substrates (Scheme 3) involving simple azides and alkynes, as well as ferrocene and steroid derivatives.

Three consecutive runs were carried out in each case. The reactions were followed by GC (Table 8, entries 1–3) and TLC measurements (entries 4–11). The products were purified by column chromatography. Good recyclability of the catalyst was observed in each case. At the same time, bulky substituents on either the alkyne or the azide components were found to retard the reaction, so triazoles **7ad**, **7ba**, **7bd** and **7ca** could be produced in moderate yields. It should be mentioned however, that from the series of compounds derived from azide **5c**, only triazole **7ca** was isolated in lower yield compared to the results obtained under homogeneous conditions.<sup>[39]</sup>

**TABLE 8** Azide–alkyne cycloaddition of various substrates<sup>a</sup>

Entry	Azide	Alkyne	Product	Yield (%) <sup>b</sup>		
				Run 1	Run 2	Run 3
1	<b>5a</b>	<b>6a</b>	<b>7aa</b>	99 (100)	98 (100)	99 (100)
2	<b>5a</b>	<b>6b</b>	<b>7ab</b>	78 (85)	70 (77)	80 (90)
3	<b>5a</b>	<b>6c</b>	<b>7ac</b>	71 (84)	76 (88)	78 (89)
4	<b>5a</b>	<b>6d</b>	<b>7ad</b>	56	41	48
5	<b>5b</b>	<b>6a</b>	<b>7ba</b>	52	50	55
6	<b>5b</b>	<b>6b</b>	<b>7bb</b>	93	91	87
7	<b>5b</b>	<b>6c</b>	<b>7bc</b>	92	96	93
8	<b>5b</b>	<b>6d</b>	<b>7bd</b>	26	24	24
9	<b>5c</b>	<b>6a</b>	<b>7ca</b>	46	45	51
10	<b>5c</b>	<b>6b</b>	<b>7cb</b>	79	76	70
11	<b>5c</b>	<b>6c</b>	<b>7cc</b>	73	70	73

<sup>a</sup>Reaction conditions: CAT-3 (10 mol% Cu), azide (0.2 mmol), alkyne (0.2 mmol), CH<sub>2</sub>Cl<sub>2</sub> (2 ml), room temperature, 24 h.

<sup>b</sup>Isolated yields after column chromatography. GC yields are in parentheses.

## 4 | CONCLUSIONS

An organic/inorganic hybrid material comprising a silica support and a polymer with imidazolium moieties was prepared for the immobilisation of a copper catalyst. The reaction conditions generally used for homogeneous reactions, such as the application of a polar solvent and the addition of a base, accelerated the reaction but also resulted in a higher loss of copper. Filtration and mercury poisoning tests showed that under these conditions both catalytically active copper complexes and nanoparticles were present in the liquid phase. By the use of a less polar solvent (CH<sub>2</sub>Cl<sub>2</sub>) and in the absence of an amine, the copper loss could be reduced considerably. The catalyst was proved to be recyclable without any loss of catalytic activity during seven consecutive runs in the reaction of phenylacetylene and benzyl azide and could be reused with good results in at least three further cycles. Recyclability was proved during the synthesis of various other triazoles, including azide and alkyne molecules with bulky substituents, such as a steroid

core or a ferrocene moiety. At the same time, steric hindrance of these groups retarded cycloaddition considerably.

## ACKNOWLEDGEMENTS

This work was supported by the National Research, Development and Innovation Office (OTKA K105632, OTKA K120014) and European Union - European Regional Development Fund (GINOP-2.3.2-15-2016-00049 grant). E.N. is grateful for the support of ÚNKP-16-2-II, New National Excellence Program of the Ministry of Human Capacities.

## ORCID

Rita Skoda-Földes <http://orcid.org/0000-0002-9810-1509>

## REFERENCES

- [1] V. V. Rostovtsev, L. G. Green, V. V. Fokin, K. B. Sharpless, *Angew. Chem. Int. Ed.* **2002**, *41*, 2596.

- [2] C. W. Tornøe, C. Christensen, M. Meldal, *J. Org. Chem.* **2002**, *67*, 3057.
- [3] H. C. Kolb, M. G. Finn, K. B. Sharpless, *Angew. Chem. Int. Ed.* **2001**, *40*, 2004.
- [4] a) C. D. Hein, X. M. Liu, D. Wang, *Pharm. Res.* **2008**, *25*, 2216. b) S. G. Agalave, S. R. Maujan, V. S. Pore, *Chem. Asian J.* **2011**, *6*, 2696.
- [5] a) H. C. Kolb, K. B. Sharpless, *Drug Discov. Today* **2003**, *8*, 1128. b) T. Efthymiou, W. Gong, J.-P. Desaulniers, *Molecules* **2012**, *17*, 12665. c) Y. M. Chabre, R. Roy, *Chem. Soc. Rev.* **2013**, *42*, 4657. d) W. Tang, M. L. Becker, *Chem. Soc. Rev.* **2014**, *43*, 7013.
- [6] L. Xu, Y. Li, Y. Li, *Asian J. Org. Chem.* **2014**, *3*, 582.
- [7] a) M. Meldal, C. W. Tornøe, *Chem. Rev.* **2008**, *108*, 2952. b) E. Haldón, M. C. Nicasio, P. J. Pérez, *Org. Biomol. Chem.* **2015**, *13*, 9528. c) M. M. Heravi, M. Tamimi, H. Yahyavi, T. Hosseinnejad, *Curr. Org. Chem.* **2016**, *20*, 1591. d) C. Wang, D. Ikhlef, S. Kahlal, J.-Y. Saillard, D. Astruc, *Coord. Chem. Rev.* **2016**, *316*, 1. e) M. S. Singh, S. Chowdhury, S. Koley, *Tetrahedron* **2016**, *72*, 5257.
- [8] a) B. Dervaux, F. E. Du Prez, *Chem. Sci.* **2012**, *3*, 959. b) A. Mandoli, *Molecules* **2016**, *21*, 1174.
- [9] a) D. Raut, K. Wankhede, V. Vaidya, S. Bhilare, N. Darwatkar, A. Deorukhkar, G. Trivedi, M. Salunkhe, *Cat. Com.* **2009**, *10*, 1240. b) A. Z. Ahmady, F. Heidarizadeh, M. Keshavarz, *Synth. Commun.* **2013**, *43*, 2100. c) S. Koguchi, K. Nakamura, *Synlett* **2013**, *24*, 2305. d) M. Javaherian, F. Kazemi, M. Ghaemi, *Chin. Chem. Lett.* **2014**, *25*, 1643.
- [10] H. Woo, H. Kang, A. Kim, S. Jang, J. C. Park, S. Park, B. S. Kim, H. Song, K. H. Park, *Molecules* **2012**, *17*, 13235
- [11] J. Y. Kim, J. C. Park, H. Kang, H. Song, K. H. Park, *Chem. Commun.* **2010**, *46*, 439.
- [12] S. Jang, Y. J. Sa, S. H. Joo, K. H. Park, *Cat. Com.* **2016**, *81*, 24.
- [13] R. Hudson, C. J. Li, A. Moores, *Green Chem.* **2012**, *14*, 622.
- [14] R. B. N. Baig, R. S. Varma, *Green Chem.* **2012**, *14*, 625.
- [15] J. M. Collinson, J. D. E. T. Wilton-Ely, S. Díez-González, *Chem. Commun.* **2013**, *49*, 11358
- [16] N. Candelon, D. Lastécouères, A. K. Diallo, J. R. Aranzaes, D. Astruc, J. M. Vincent, *Chem. Commun.* **2008**, 741.
- [17] B. H. Lipshutz, B. R. Taft, *Angew. Chem. Int. Ed.* **2006**, *45*, 8235.
- [18] H. López-Ruiz, J. E. Cerda-Pedro, S. Rojas-Lima, I. Pérez-Pérez, B. V. Rodríguez-Sánchez, R. Santillan, O. Coreño, *ARKIVOC* **2013**, *3*, 139.
- [19] V. H. Reddy, Y. V. R. Reddy, B. Sridhar, B. V. S. Reddy, *Adv. Synth. Catal.* **2016**, *358*, 1088.
- [20] T. Katayama, K. Kamata, K. Yamaguchi, N. Mizuno, *ChemSusChem* **2009**, *2*, 59.
- [21] S. Chassaing, A. S. S. Sido, A. Alix, M. Kumarraja, P. Pale, J. Sommer, *Chem. A Eur. J.* **2008**, *14*, 6713.
- [22] B. J. Borah, D. Dutta, P. P. Saikia, N. C. Barua, D. K. Dutta, *Green Chem.* **2011**, *13*, 3453.
- [23] H. Hagiwara, H. Sasaki, T. Hoshi, T. Suzuki, *Synlett* **2009**, 643.
- [24] P. Li, L. Wang, Y. Zhang, *Tetrahedron* **2008**, *64*, 10825
- [25] R. B. N. Baig, R. S. Varma, *Green Chem.* **2013**, *15*, 1839.
- [26] M. Chetia, A. A. Ali, D. Bhuyan, L. Saikia, D. Sarma, *New J. Chem.* **2015**, *39*, 5902.
- [27] C. Girard, E. Xnen, M. Aufort, S. Beauvière, E. Samson, J. Herscovici, *Org. Lett.* **2006**, *8*, 1689.
- [28] T. R. Chan, V. V. Fokin, *QSAR Comb. Sci.* **2007**, *26*, 1274.
- [29] U. Sirion, Y. J. Bae, B. S. Lee, D. Y. Chi, *Synlett* **2008**, *15*, 2326.
- [30] L. Bonami, W. V. Camp, D. V. Rijckegem, F. E. D. Prez, *Macromol. Rapid Commun.* **2009**, *30*, 34.
- [31] S. I. Presolski, S. K. Mamidyala, F. Manzenrieder, M. G. Finn, *ACS Comb. Sci.* **2012**, *14*, 527.
- [32] E. Ozkal, S. Ozcubukcu, C. Jimeno, M. A. Perics, *Cat. Sci. Technol.* **2012**, *2*, 195.
- [33] Y. M. A. Yamada, S. M. Sarkar, Y. Uozumi, *J. Am. Chem. Soc.* **2012**, *134*, 9285.
- [34] X. Liu, N. Novoa, C. Manzur, D. Carrillo, J. R. Hamon, *New J. Chem.* **2016**, *40*, 3308.
- [35] G. M. Pawar, B. Bantu, J. Weckesser, S. Blechert, K. Wurst, M. R. Buchmeiser, *Dalton Trans.* **2009**, 9043.
- [36] A. Alix, S. Chassaing, P. Pale, J. Sommer, *Tetrahedron* **2008**, *64*, 8922.
- [37] K. Fehér, Á. Gömöry, R. Skoda-Földes, *Monatsh. Chem.* **2015**, *146*, 1455.
- [38] E. Szánti-Pintér, J. Balogh, Z. Csók, L. Kollár, Á. Gömöry, R. Skoda-Földes, *Steroids* **2011**, *76*, 1377.
- [39] K. Fehér, J. Balogh, Z. Csók, T. Kégl, L. Kollár, R. Skoda-Földes, *Steroids* **2012**, *77*, 738.
- [40] a) T. Romero, A. Caballero, A. Tárraga, P. Molina, *Org. Lett.* **2009**, *11*, 3466. b) T. Romero, R. A. Orenes, A. Espinosa, A. Tárraga, P. Molina, *Inorg. Chem.* **2011**, *50*, 8214. c) F. Oton, M. C. Gonzalez, A. Espinosa, A. Tárraga, P. Molina, *Organometallics* **2012**, *31*, 2085. d) F. Oton, M. C. Gonzalez, A. Espinosa, C. Ramirez de Arellano, A. Tárraga, P. Molina, *J. Org. Chem.* **2012**, *77*, 10083. e) T. Romero, R. A. Orenes, A. Tárraga, P. Molina, *Organometallics* **2013**, *32*, 5740. f) M. C. Gonzalez, F. Oton, R. A. Orenes, A. Espinosa, A. Tárraga, P. Molina, *Organometallics* **2014**, *33*, 2837.
- [41] a) P. Nnane, V. C. O. Njar, A. A. Brodie, *J. Steroid Biochem. Mol. Biol.* **2001**, *78*, 241. b) Z. Kádár, D. Kovács, É. Frank, G. Schneider, J. Huber, I. Zupkó, T. Bartók, J. Wölfling, *Molecules* **2011**, *16*, 4786. c) R. C. N. R, N. B. Corrales, L. S. De Souza, C. Pinheiro, E. S. Abramo, A. D. D. S. Coimbra, *Biomed. Pharmacother.* **2011**, *65*, 198.
- [42] S. Letaief, J. Leclercq, Y. Liu, C. Detellier, *Langmuir* **2011**, *27*, 15248
- [43] M. K. Barman, A. K. Sinha, S. Nembenna, *Green Chem.* **2016**, *18*, 2534.
- [44] E. Ozkal, P. Llanes, F. Bravo, A. Ferrali, M. A. Pericàs, *Adv. Synth. Catal.* **2014**, *356*, 857.
- [45] F. Alonso, Y. Moglie, G. Radivoy, M. Yus, *Eur. J. Org. Chem.* **2010**, 1875.
- [46] Y. Wang, J. Liu, C. Xia, *Adv. Synth. Catal.* **2011**, *353*, 1534.
- [47] C. D. Wagner, W. M. Riggs, L. E. Davis, J. F. Moulder, G. T. Muilenberg, *Handbook of X-Ray Photoelectron Spectroscopy*,

- Perkin-Elmer Corporation, Physical Electronics Division, Eden Prairie, MN **1979**.
- [48] C. D. Wagner, A. V. Naumkin, A. Kraut-Vass, J. W. Allison, C. J. Powell, J. R. Rumble Jr, NIST Standard Reference Database 20, Version 3.4 (web version), **2003** (<http://srdata.nist.gov/xps/>)
- [49] M. C. Biesinger, L. W. M. Laua, A. R. Gerson, R. S. C. Smart, *Appl. Surf. Sci.* **2010**, 257, 887.
- [50] F. Truica-Marasescu, M. R. Wertheimer, *Plasma Processes Polym.* **2008**, 5, 44.
- [51] D. Briggs, D. M. Brewis, R. H. Dahm, I. W. Fletcher, *Surf. Interface Anal.* **2003**, 35, 156.
- [52] A. G. Shard, J. D. Whittle, A. J. Beck, P. N. Brookes, N. A. Bullett, R. A. Talib, A. Mistry, D. Barton, S. L. McArthur, *J. Phys. Chem. B* **2004**, 108, 12472
- [53] T. H. Lippert, F. Zimmermann, A. Wokaun, *Appl. Spectrosc.* **1993**, 47, 1931.
- [54] G. Beamson, D. Briggs, *High Resolution XPS of Organic Polymers—The Scienta ESCA300 Database*, Wiley Interscience **1992**.

## SUPPORTING INFORMATION

Additional Supporting Information may be found online in the supporting information tab for this article.

**How to cite this article:** Fehér K, Nagy E, Szabó P, et al. Heterogeneous azide–alkyne cycloaddition in the presence of a copper catalyst supported on an ionic liquid polymer/silica hybrid material. *Appl Organometal Chem.* 2018;e4343. <https://doi.org/10.1002/aoc.4343>